

# A Multi-Scale Boltzmann Equation for Complex Systems of Neutral Gases across All Flow Regimes

Sha Liu<sup>1,2,\*</sup>, Junzhe Cao<sup>1,†</sup>, Sirui Yang<sup>1,‡</sup> and Chengwen Zhong<sup>1,2,§</sup>

*1 National Key Laboratory of Science and Technology on Aerodynamic Design and Research, Northwestern Polytechnical University, Xi'an, Shaanxi, China*

*2 Institute of Extreme Mechanics, Northwestern Polytechnical University, Xi'an, Shaanxi, China*

(Dated: June 12, 2024)

A Multi-scale Boltzmann Equation (MBE) is found from the gas-kinetic theory and the direct modeling philosophy as a master equation for complex physical systems of neutral gases across all flow regimes, which locates between the continuum limit and the free-molecular limit, covering a vast range of applications such as hypersonic flows over aerospace crafts and delicate flows around MEMS. The most explicit characteristic of MBE is evolving the variable observation time in the expression, which distinguishes the MBE from the single-scale master or governing equation where a fixed scale is implied in the assumptions. The fundamental properties of MBE, such as the asymptotic property, are proved theoretically, while a concise numerical scheme is developed for MBE to demonstrate its validity by benchmark multi-scale problems.

At the present stage, more and more important physics areas and disciplines can be classified as the multi-scale physics or complex physical systems, such as the nuclear physics[1], the plasma[2, 3], the atmosphere[4] and the transitional gas flows[5]. The scales of these phenomena often extend beyond the scope of mature theories, which are specific to single scales. This results in knowledge gaps regarding multi-scale physical mechanisms and the lack of determined multi-scale master equations.

In the complex system of neutral gases across all flow regimes between the macroscopic continuum limit and the microscopic free-molecular limit, the challenge of undetermined physical mechanisms is tackled through either the rough averaging of micro-scale information for macro-scale governing equations[6] or the coupling of microscopic and macroscopic mechanisms using specific physical principles[7–9] and model equations[10–14]. Additionally, some approaches attempt to tackle this issue through a mathematical synthetic iteration[15] of equations across different scales. While, in the same situation as many other physical fields, there lacks the important master equation based on which the theory and numerical method of a given complex physical system can be established concretely and providing a steady and rational foundation for the above treatments. In this paper, we aim to find a multi-scale master equation for the complex system of neutral gases.

In the complex system of neutral gases, the continuum limit and continuum flows are described by the aerodynamics and Navier-Stokes (N-S) governing equations, and the free molecular limit and rarefied flows are described by the gas kinetic theory and the Boltzmann equation. Therefore a multi-scale equation should bridge the gap

between the two limits and can also recover the two limits with the Asymptotic Preserving (AP) property[16].

As is well known, the Boltzmann Equation (BE)[17] serves as the master equation of gas-kinetic theory, which is a single scale equation whose spatial and temporal scales are the mean free path and the mean collision time of molecules, respectively. Its differential-(nonlinear five-fold) integral mathematical form is as follows:

$$\frac{\partial f}{\partial t} + \boldsymbol{\xi} \cdot \frac{\partial f}{\partial \mathbf{x}} = \int_{R^3} \int_0^{4\pi} (f'_1 f' - f_1 f) \xi_r \sigma d\Omega d\boldsymbol{\xi}_1, \quad (1)$$

where  $f(\mathbf{x}, \boldsymbol{\xi}, t)$  is the molecular distribution,  $\mathbf{x}$  is the location,  $t$  is the time,  $\boldsymbol{\xi}$  is the molecular velocity ( $\mathbf{x}$  and  $\boldsymbol{\xi}$  are omitted for simplicity in the following pages).  $\xi_r = |\boldsymbol{\xi} - \boldsymbol{\xi}_1|$ ,  $\sigma$  and  $\Omega$  are the relative velocity, differential cross section, and solid angle. The distribution with prime denotes the after-collision one, and the distribution with subscript “1” is for velocity  $\boldsymbol{\xi}_1$ . The left-hand side of Eq. 1 denotes the free-transport of particles, and the right-hand side denotes the collision term, briefly noted by  $B(f, f)$ .

To examine the Boltzmann equation from a multi-scale perspective, we require some fundamental principles that hold across all scales, such as the second law of thermodynamics. Therefore, a multi-scale temporal integral solution is introduced, which describes the trend of a random distribution (system) towards the equilibrium, and can be written as follows:

$$f(t + \Delta t) = e^{-\frac{\Delta t}{\tau}} f(t) + \left(1 - e^{-\frac{\Delta t}{\tau}}\right) g(t), \quad (2)$$

where  $\Delta t$  is the observation scale,  $\tau = \mu/p$  is the relaxation time, here  $\mu$  is the viscosity coefficient,  $g$  is the local equilibrium distribution function in the following form:

$$g = n \left( \frac{m}{2\pi kT} \right)^{\frac{3}{2}} \exp \left( - \frac{m(\boldsymbol{\xi} - \mathbf{U}) \cdot (\boldsymbol{\xi} - \mathbf{U})}{2kT} \right), \quad (3)$$

where  $m$  is the molecular mass,  $k$  is the Boltzmann constant.  $n$ ,  $\mathbf{U}$ ,  $T$  are macroscopic number density, velocity

\* shaliu@nwpu.edu.cn

† caojunzhe@mail.nwpu.edu.cn

‡ yrsr1997@mail.nwpu.edu.cn

§ Corresponding author: zhongcw@nwpu.edu.cn

and temperature. This temporal integral solution can be obtained from the Bhatnagar-Gross-Krook (BGK) model of Boltzmann equation, whose collision term also directly describes the trend of non-equilibrium distribution towards the equilibrium one.

Since  $f(t + \Delta t)$  from the multi-scale temporary integral solution (Eq. 2) follows the original Boltzmann equation as an ordinary distribution function, by substituting it into the original Boltzmann equation (Eq. 1), the Boltzmann equation turns into:

$$\begin{aligned} e^{-\Delta t/\tau} \frac{Df}{Dt} + \left(1 - e^{-\Delta t/\tau}\right) \frac{Dg}{Dt} \\ = e^{-\Delta t/\tau} \left(1 - e^{-\Delta t/\tau}\right) [B(g, f) + B(f, g)] \quad (4) \\ + e^{-2\Delta t/\tau} B(f, f) + \left(1 - e^{-\Delta t/\tau}\right)^2 B(g, g). \end{aligned}$$

Given that the collision term for equilibrium state  $g$  vanishes:

$$\frac{Dg}{Dt} = B(g, g) \equiv 0, \quad (5)$$

after simplifications, the resultant equation becomes:

$$\frac{Df}{Dt} = e^{-\frac{\Delta t}{\tau}} B(f, f) + \left(1 - e^{-\frac{\Delta t}{\tau}}\right) \{B(f, g) + B(g, f)\}, \quad (6)$$

where  $\{B(f, g) + B(g, f)\}$  is just the collision term of the Linearized Boltzmann Equation (LBE) [18]. By denoting the linearized Boltzmann collision term by  $L(f)$ , the resultant equation can be further written as:

$$\frac{Df}{Dt} = e^{-\frac{\Delta t}{\tau}} B(f, f) + \left(1 - e^{-\frac{\Delta t}{\tau}}\right) L(f). \quad (7)$$

The assumption of linearized Boltzmann equation is that the distribution function is not far from equilibrium, and  $L(f)$  describes the molecular collisions when  $\Delta t \gg \tau$  in/near the continuum flow regime. In this work, Eq. 7 is called the Multi-scale Boltzmann Equation (MBE), which is obtained through the above process that investigates the microscopic Boltzmann equation from a multi-scale perspective. Examining this equation, some useful property can be identified:

- (1) The observation time  $\Delta t$  is introduced into the master equation (Eq. 7).  $\Delta t/\tau$  in the exponential is physically the ratio of observation time scale to the molecular transportation time scale, where  $\Delta t$  can variate from microscopic to macroscopic.
- (2) The multi-scale collision term of MBE is a convex combination (weighted average) of the BE one and the LBE one, and it covers the whole flow regime between the continuum limit and free-molecular limit.

It is evident that the MBE equation has the correct Chapman-Enskog (C-E) expansion (AP property), since

both BE and LBE have this property and MBE is their linear combination. For the same reason, the MBE also satisfies the basic H theorem (the second law of thermodynamics in gas-kinetic theory) and the conservation of collision invariants.

Two types of interpretations of MBE collision term can be made as follows: one is the molecules have a weighted collision term during the whole observation time  $\Delta t$ . This indirectly corroborates some numerical methods for Boltzmann equation in large time step[7, 8]. The other interpretation is a two time step process that molecules follow the BE collision term during  $\delta t_1 = e^{-\Delta t/\tau} \Delta t < \tau$ , and follow LBE collision term during  $\delta t_2 = (1 - e^{-\Delta t/\tau}) \Delta t$ . Given the first (order) term of  $L(f)$  is a BGK collision term[18],  $L(f)$  can be approximated by the relaxation collision term  $R(f) = (g - f)/\tau$  during  $\delta t_2$ , and the Quantified Model Competition (QMC) mechanism[19] for large temporal scale can be used, where a molecule is randomly classified as a free transport one or a colliding one, with the probabilities  $e^{-\frac{\delta t_2}{\tau}}$  and  $(1 - e^{-\frac{\delta t_2}{\tau}})$ , respectively, as follows:

$$f(\Delta t) = e^{-\frac{\delta t_2}{\tau}} f_{BE} + \left(1 - e^{-\frac{\delta t_2}{\tau}}\right) f_{CE}, \quad (8)$$

where  $f_{BE}$  is the distribution function after  $\delta t_1$  and  $f_{CE}$  is the second order C-E distribution,  $f_{CE} = Dg/Dt + \xi \cdot \partial g/\partial \mathbf{x}$ . Eq. 8 is obtained by spatial and temporal Taylor expansion of the temporal integral solution of an inhomogeneous BGK equation during  $\delta t_2$ [19]. Eq. 8 can also be viewed as a formal solution of MBE describing that, after an evolution during  $\Delta t$ ,  $e^{-\delta t_2/\tau}$  portion of molecules experience a BE process, while  $1 - e^{-\delta t_2/\tau}$  portion of molecules follow the second order CE distribution corresponding to the macroscopic N-S equation.

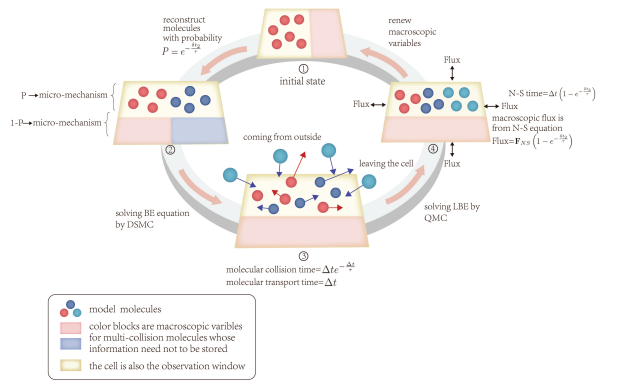


FIG. 1. The two-step process for MBE solver.

Given the two steps of the MBE process, a concise numerical algorithm for MBE can be formulated as follows, as illustrated in Fig. 1. The flow field is discretized into discrete cells (volumes). Model molecules are employed to describe the non-equilibrium distribution function from  $f_{BE}$ , each representing a large amount

of real molecules[20]. Meanwhile, the near-equilibrium part of distribution function  $f_{CE}$  is entirely determined by macroscopic variables.

**Step 1:** At the beginning of a new time step, there are free transport molecules and macroscopic variables representing the colliding molecules from the previous time step. They will be re-categorized in this new time step: The previous free transport molecules are reclassified as candidate free transport and candidate colliding molecules during the large temporal process in  $\delta t_2$ , with different probabilities (weights)  $e^{-\delta t_2/\tau}$  and  $1 - e^{-\delta t_2/\tau}$ . Since the second order C-E distribution corresponds to the macroscopic N-S equation and is fully determined by the macroscopic variables, the transport of all colliding molecule in cell can be represented by the macroscopic N-S equation. Their individual information can be erased and merged into the macroscopic variables. On the other hand, some molecules will emerge from the local Maxwellian distribution, determined by the previous macroscopic variables, with a probability  $e^{-\delta t_2/\tau}$ .

**Step 2:** For numerically solving the BE equation during  $\delta t_1$ , the DSMC method[20] is adopted, which involves splitted and successive free transport and collision processes. In the MBE solver, DSMC collisions are calculated during  $\delta t_1$  for model molecules in cell, while their transport time is  $\Delta t$ , since these model molecules are free transport molecules during  $\delta t_2$ . The mature No-Time Counter (NTC) collision method is chosen, which has the classic collision process, whose details can be found in Ref.[20].

**Step 3:** The N-S equation is solved using an ordinary Computational Fluid Dynamics (CFD) method[21, 22]. The overall macroscopic flux of colliding molecules is calculated from the numerical flux of the N-S equation while multiplying by their scale weight  $1 - e^{-\delta t_2/\tau}$  (The treatment of the flux at the boundary is the same). In this paper, the Kinetic Inviscid Flux (KIF) which is convenient for multi-scale frameworks is selected[23].

**Step 4:** Finally, total macroscopic variables in cell can be updated as follows:

$$\begin{aligned} \mathbf{W}^{n+1} = & \mathbf{W}^n - \mathbf{W}_{DSMC}^n + \mathbf{W}_{DSMC}^{n+1} \\ & + \left(1 - e^{-\frac{\delta t_2}{\tau}}\right) \sum_{cf=1}^{cfn} \mathbf{F}_{NS} \cdot \mathbf{S}_{cf} \Delta t, \end{aligned} \quad (9)$$

where,  $\mathbf{W}$  is the macroscopic conservation field variables cumulated in cell (volume)  $\Omega$  as  $\mathbf{W} = (\rho\Omega, \rho\mathbf{U}\Omega, \rho U^2\Omega + 3\rho RT\Omega)^T$ , the superscripts  $n$  and  $n+1$  indicate the iteration time steps.  $\mathbf{S}_{cf}$  is the directed

area pointing out of a cell.  $cfn$  is the number of cell interfaces. It can be found that a MBE solver only unifies the DSMC and N-S solvers by the scale-dependent weights, and both algorithms are unchanged.

An important detail should be mentioned: Since meshes vary significantly in different locations of a flow field, a local and physical time is used to determine the observation scale in each cell, which is  $\Delta t_{phy} = L_{cell}/u_{cell}$ , where  $L_{cell}$  can be the cubic root of a cell volume and  $u_{cell}$  can be  $|U| + \sqrt{\gamma RT}$ . Therefore, the  $L_{cell}$  and  $\Delta t_{phy}$  are the observation length and time scales for this discrete cell, which fits the essence of mesh resolution quite physically. The  $\Delta t_{phy}$  for all cells is only used for calculating the scale weights. The numerical process proceeds in the numerical time step  $\Delta t$  which is the smallest  $\Delta t_{phy}$  in the flow field.

To test the validity and accuracy of the MBE, as well as the numerical solver, a normal shock wave is first calculated near two scale limits. The upstream Mach number (Ma) is set to be 3. The working gas is argon, and the Variable Hard Sphere (VHS) model[20] is used with  $\omega = 0.5$ . The observation scale is zoomed into the internal of shock wave from the macro-one to the micro-one. In Fig.2, the MBE numerical solution matches well with those of the N-S equation in continuum region ( $\Delta x = 10^5 \lambda$ ) and DSMC solutions[24] in rarefied region ( $\Delta x = \lambda/4$ ), respectively. Here  $\lambda$  is the molecular mean free path in the upstream.

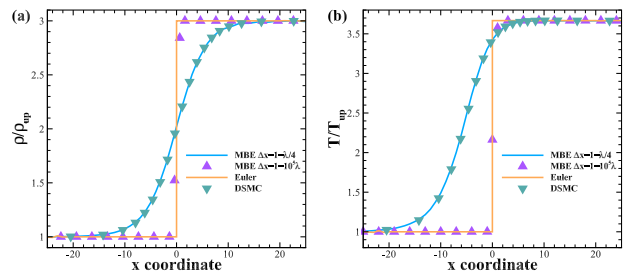


FIG. 2. Density and temperature profiles in the internal of a  $Ma = 3$  shock wave.

A more scale-sensitive case is the hypersonic cylinder flow in the transitional inflow condition[25, 26] ( $Ma = 5$ ,  $Kn = \frac{\lambda}{L} = 0.01$ , the inflow temperature  $T_\infty$  is the same as wall temperature  $T_w$ ). The working gas is argon. The VHS model is used with  $\omega = 0.81$ ). As shown in Fig.3, the flow scale changes significantly in a single flow field. The DSMC solution with extremely small mesh cells (to satisfy the condition  $L_{cell} \leq \lambda/3$ ) with huge computational cost is used as the benchmark solution. The detailed macroscopic variables at the stagnation (central horizontal) line and the sensitive viscous heat flux and shear stress along the cylinder surface are illustrated in Fig.3. The results of MBE solver match well with the benchmark solution. Notice that, since the resolution of MBE solver is not limited by the microscopic spatial scale (such as  $\lambda/3$ ), its mesh can be set according to the

slopes of the flow field. The computational cost of both methods is presented in Tab.I. The number of collision cells of DSMC is about 2.7 million, and the cell number of MBE solver is about 17.9 thousand. The efficiency is often a crucial advantage of multi-scale methods.

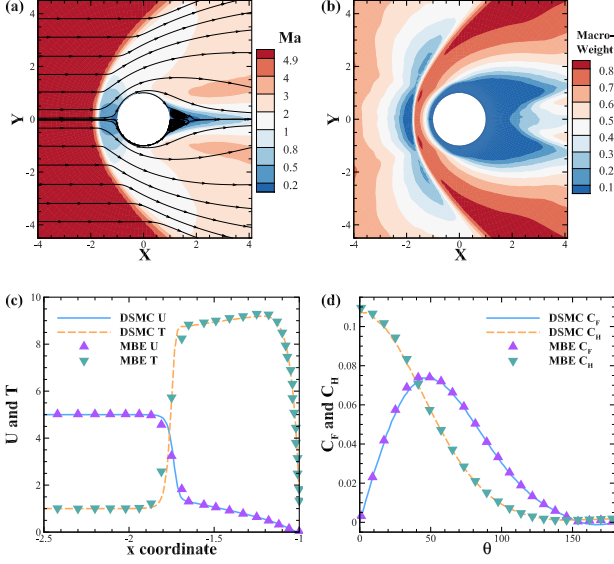


FIG. 3. Results of argon gas cylinder flow at  $Ma = 5$ ,  $Kn = 0.01$ : (a) Ma contour, (b) macro-weight contour calculated by  $(1 - e^{-\delta t_2/\tau})$ , (c) velocity and temperature at the stagnation line, the reference values are  $\sqrt{\gamma RT_\infty}$  and  $T_\infty$ , respectively, (d) shear stress and heat flux on the solid wall, the reference values are  $0.5\rho_\infty U_\infty^2$  and  $0.5\rho_\infty U_\infty^3$ , respectively.

TABLE I. Comparisons of the DSMC solver and MBE solver

	DSMC	MBE
Particle number (million)	21.3	3.3
Executive time (h)	122.7	24.7

A more challenging case is the jet flow into a vacuum environment, which is significant for aircrafts and MEMS applications. For this unsteady case, the physical scale not only varies across the flow field but also varies with time. In Ref.[27], this type of flow is specially studied, and a classical condition is applied to validate the present MBE. The inflow  $Ma$  is 2.19, and  $Kn$  is  $10^{-4}$ , whose reference length is the nozzle width  $L = 1$ . The inflow temperature  $T_{in}$  is the same as the wall temperature  $T_w$ . The working gas is argon, and VHS model is used with  $\omega = 0.81$ . The results near the starting time ( $t = 0.5, t_{ref} = L/\sqrt{RT_{in}}$ ) and at steady state are shown in Fig.4. The density fields predicted by MBE solver (exhibited by contour) are in line well with benchmark solutions (exhibited by dash line).

For 3D cases, the hypersonic sphere in all flow regimes is considered. In this case, the inflow  $Ma$  is 3, and  $Kn$  varies from  $10^{-3}$  to 10. The inflow temperature is iden-

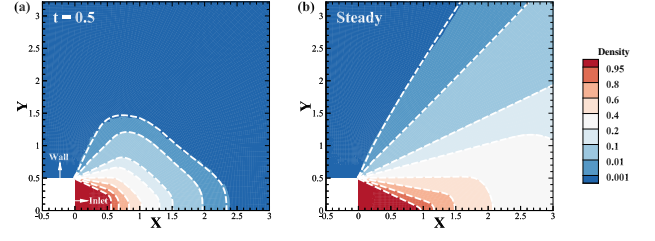


FIG. 4. Result of jet flow into vacuum (The density fields predicted by MBE solver are exhibited by contour and benchmark solutions are exhibited by line): (a) Near the start time ( $t = 0.5, t_{ref} = L/\sqrt{RT_{in}}$ ), (b) steady time.

tical to the wall temperature. The working gas is argon, and VHS model is used with  $\omega = 0.81$ . The drag coefficients are summarized and closely match the results obtained from DSMC simulations, as shown in Fig.5. The detailed values are exhibited in Tab.II. To obtain a compromise benchmark data, the DSMC is also used in the low  $Kn$  case, despite of the huge computational cost.

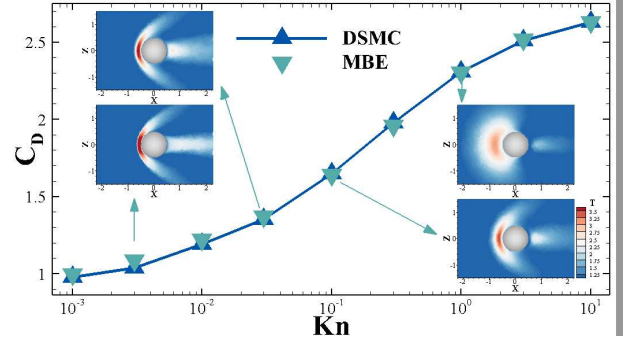


FIG. 5. Drag coefficients of supersonic sphere flow at  $Ma = 3$ .

TABLE II. Comparison of drag coefficients between the DSMC solver and MBE solver

$Kn$	0.001	0.003	0.01	0.03	0.1	0.3	1	3	10
DSMC	0.98	1.04	1.19	1.35	1.65	1.98	2.31	2.51	2.63
MBE	1.00	1.09	1.22	1.37	1.64	1.96	2.30	2.52	2.63

In summary, the MBE is found for the complex system of neutral gas flows across all flow regimes, which is physically a scale-dependent convex combination of the single-scale BE for rarefied flows and the LBE in the near continuum regime. Benefitting from the clear physical picture of MBE, a concise numerical solver is developed which is simply the unification of the rarefied DSMC solver and the continuum N-S solver, gaining a concrete multi-scale ability. The validity of MBE and efficiency of its numerical solver are proved in the above benchmark and challenging test cases. Finally, we hope the process of finding multi-scale master equations for complex physical system in this work to be useful for other multi-scale physics and science areas.

This work is supported by National Natural Science Foundation of China (12172301, 12072283).

- 
- [1] J. Jia, G. Giacalone, and C. Zhang, Separating the impact of nuclear skin and nuclear deformation in high-energy isobar collisions, *Physical Review Letters* **131**, 022301 (2023).
- [2] W. Bin, C. Castaldo, F. Napoli, P. Buratti, A. Cardinali, A. Selce, and O. Tudisco, First intrashot observation of runaway-electron-driven instabilities at the lower-hybrid frequency range under ITER-relevant plasma-wave dispersion conditions, *Physical Review Letters* **129**, 045002 (2022).
- [3] C. Brée, M. Hofmann, A. Demircan, U. Morgner, O. Kosareva, A. Savel'ev, M. Hussakou, A. Ivanov, and I. Babushkin, Symmetry breaking and strong persistent plasma currents via resonant destabilization of atoms, *Physical Review Letters* **119**, 243202 (2017).
- [4] B. Andreotti, A. Fourrière, F. Ould-Kaddour, B. Murray, and P. Claudin, Giant aeolian dune size determined by the average depth of the atmospheric boundary layer, *Nature* **457**, 1476 (2009).
- [5] M. A. Gallis, N. P. Bitter, K. T. P., J. R. Torczynski, S. J. Plimpton, and G. Papadakis, Molecular-level simulations of turbulence and its decay, *Physical Review Letters* **118**, 064501 (2017).
- [6] M. Torrilhon, Modeling nonequilibrium gas flow based on moment equations, *Annual Review of Fluid Mechanics* **48**, 429 (2016).
- [7] E. Gabetta, L. Pareschi, and G. Toscani, Relaxation schemes for nonlinear kinetic equations, *SIAM Journal on Numerical Analysis* **34**, 2168 (1997).
- [8] W. Ren, H. Liu, and S. Jin, An asymptotic-preserving Monte Carlo method for the Boltzmann equation, *Journal of Computational Physics* **276**, 380 (2014).
- [9] N. Yang, W. Wang, W. Ge, and J. Li, CFD simulation of concurrent-up gas-solid flow in circulating fluidized beds with structure-dependent drag coefficient, *Chemical Engineering Journal* **96**, 71 (2003).
- [10] K. Xu and J.-C. Huang, A unified gas-kinetic scheme for continuum and rarefied flows, *Journal of Computational Physics* **229**, 7747 (2010).
- [11] Z. Guo, K. Xu, and R. Wang, Discrete unified gas kinetic scheme for all knudsen number flows: Low-speed isothermal case, *Physical Review E* **88**, 033305 (2013).
- [12] Z. Li and H. Zhang, Study on gas kinetic unified algorithm for flows from rarefied transition to continuum, *Journal of Computational Physics* **193**, 708 (2004).
- [13] L. M. Yang, C. Shu, W. M. Yang, and J. Wu, An improved three dimensional implicit discrete velocity method on unstructured meshes for all Knudsen number flows, *Journal of Computational Physics* **396**, 738 (2019).
- [14] C. Liu, Y. Zhu, and K. Xu, Unified gas-kinetic wave-particle methods I: Continuum and rarefied gas flow, *Journal of Computational Physics* **401**, 108977 (2020).
- [15] W. Su, L. Zhu, P. Wang, Y. Zhang, and L. Wu, Can we find steady-state solutions to multiscale rarefied gas flows within dozens of iterations?, *Journal of Computational Physics* **407**, 109245 (2020).
- [16] E. W. Larsen and J. B. Keller, Asymptotic solution of neutron transport problems for small mean free paths, *Journal of Mathematical Physics* **15**, 75 (1974).
- [17] S. Chapman and C. T. G., *The mathematical theory of non-uniform gases* (Cambridge University Press, 1970).
- [18] C. Cercignani, *Mathematical methods in kinetic theory* (Plenum Press, 1969).
- [19] S. Liu, C. Zhong, and M. Fang, Simplified unified wave-particle method with quantified model-competition mechanism for numerical calculation of multiscale flows, *Physical Review E* **102**, 013304 (2020).
- [20] G. A. Bird, *Molecular gas dynamics and the direct simulation of gas flows* (Clarendon Press, 1994).
- [21] C. Hirsch, *Numerical computation of internal and external flows* (Elsevier, 2007).
- [22] R. J. LeVeque, *Finite volume methods for hyperbolic problems* (Cambridge university press, 2002).
- [23] S. Liu, J. Cao, and C. Zhong, Multiscale kinetic inviscid flux extracted from a gas-kinetic scheme for simulating incompressible and compressible flows, *Physical Review E* **102**, 033310 (2020).
- [24] T. Ohwada, Structure of normal shock waves: Direct numerical analysis of the Boltzmann equation for hard-sphere molecules, *Physics of Fluids A: Fluid Dynamics* **5**, 217 (1993).
- [25] A. J. Lofthouse, *Nonequilibrium hypersonic aerothermodynamics using the direct simulation Monte Carlo and Navier-Stokes models*, Ph.D. thesis, University of Michigan (2008).
- [26] F. Fei, A time-relaxed Monte Carlo method preserving the Navier-Stokes asymptotics, *Journal of Computational Physics* **486**, 112128 (2023).
- [27] J. Chen, S. Liu, Y. Wang, and C. Zhong, A compressible conserved discrete unified gas-kinetic scheme with unstructured discrete velocity space for multi-scale jet flow expanding into vacuum environment, *Communications in Computational Physics* **28**, 1502 (2020).